RESILIENT INFRASTRUCTURE
June 1–4, 2016
RESILIENT INFRASTRUCTURE LONDON 2016

IMPACT OF SLENDERNESS ON THE SEISMIC RESPONSE OF ROCKING FRAMES IN ONTARIO NUCLEAR POWER PLANTS

Amitabh Dar
Technical Advisor, Bruce Power, Canada
Doctoral Researcher, McMaster University, Canada

Dimitrios Konstantinidis
Assistant Professor, McMaster University, Canada

Wael El-Dakhakhni
Associate Professor, McMaster University, Canada
Martini, Mascarin and George Chair in Masonry Design, McMaster University, Canada

ABSTRACT

Canadian Nuclear Power Plants (NPPs) are located on the eastern side of the North American continent, with the majority of them in Ontario. The Design Basis Earthquake (DBE), based on West Coast records, is prescribed in the Canadian nuclear standards. Seismic Probabilistic Risk Assessment studies of the existing plants consider time histories obtained from the latest research on the East Coast earthquakes as seismic input to the analysis. Although Canadian standards are silent about rocking response of unanchored objects, various industry guidelines and the standard ASCE 43-05 prescribe methodologies in this regard. Applications of a rocking frame in a NPP may vary from squat piers supporting a heavy rigid object to a slender masonry frame consisting of two concrete block walls and a rigid diaphragm on top. The methods of analysis prevalent in the nuclear industry recommend obtaining the response of an *individual* pier of a rocking frame, rather than an *equivalent* pier representing the rocking frame. Methods of obtaining an equivalent pier, whose response is the same as that of a rocking frame, have been detailed in the literature where it has been emphasized that rocking frames are more stable than an individual rocking pier. However, it is noticed that the response of rocking frames is influenced by their slenderness and also by the boundary condition at the contact between the piers and the top mass. The support boundary conditions are bounded by two extremes: the full top width of a pier, or a point support at its top center. This paper compares the equivalent block parameters of rocking frames for these two extreme boundary conditions. Also, it presents the seismic response of a slender rocking frame subjected to earthquake records compatible with the DBE spectra of Ontario NPPs, as well as spectra used in risk analysis.

Keywords: Nuclear, Seismic, Rocking, Frame, DBE, CSA.

1. INTRODUCTION

Ontario NPPs, being closer to the east coast in comparison to the west, are considered as East Coast plants subject to high frequency seismic excitation typically represented by the East North American (ENA) response spectrum (Atkinson and Elgohary, 2007). Many eastern Canadian moderate earthquakes, including the classic Saguenay (1988) earthquake were found to be rich in high frequency content (Boore and Atkinson, 1992). The seismic design response spectrum in the United States Nuclear Regulatory Commission (USNRC) Regulatory Guide (RG) 1.60 (USNRC, 1973) was based on the NBK spectrum (Newmark et al., 1973), named after its creators and generated from the West Coast strong motion records. The standard response spectrum in the Canadian nuclear code CSA N289.3 (1981) was based on the USNRC regulatory document NUREG CR-0098 (Newmark and Hall, 1978) that considered the seismic input from the West Coast records. Both USNRC RG 1.60 (1973) and CSA N289.3 (1981) recommended their respective generic spectra to be scaled to suit the site-specific Peak Ground Acceleration (PGA). The newer versions of these publications USNRC RG 1.60, Revision 2 (USNRC, 2014), and CSA N289.3 (2010) include

recommendations about the high frequency events. However, the shapes of the generic spectra remain the same as in the older versions. The DBEs of the Ontario NPPs are either scaled versions of the NBK spectrum or the CSA spectrum. Figure 1 illustrates the difference between the two. For the purpose of Seismic Margin Assessment (SMA) of an Ontario NPP, East Coast events (richer in high frequency content) are considered in order to establish the Uniform Hazard Response Spectrum (UHRS) required as the basis of the SMA (Alexander et al., 2007). Seismic Probabilistic Risk Assessment also requires generation of UHRS which is based on the East Coast events for Ontario NPPs. Discussion on the comparison of shapes of various design basis spectra and the assessment spectra can be found elsewhere (e.g., Dar et al., 2015a). For the purpose of this paper, four earthquake records are considered, out of which, three are common or similar to the records in (Newmark et al., 1973) and (Newmark and Hall, 1978), and one is from the suite of Saguenay records as a representative of typical Canadian East Coast events with high frequency content.

Seismic interaction of unanchored objects, with seismically qualified safety systems, may adversely impact their capability to perform their intended functions, and hence it is required to be assessed in accordance with the Electric Power and Research Institute (EPRI) report NP-6041 (EPRI, 1991). The response of a rocking object has not been addressed in the Canadian nuclear standards (Dar et al., 2013). In this regard a designer has to refer to the available literature or standards in the nuclear industry outside Canada. The standard ASCE 43-05 states that it is preferable to anchor components in an NPP to avoid rocking and sliding. However, unanchored components are acceptable as long as they satisfy the requirements of the standard. Components such as portable power supply, transformers, tooling cabinets etc. cannot be anchored to the floor because of their frequent movement. Structural components such as concrete shielding blocks or unreinforced masonry (URM) are potential candidates for their seismic interaction with the surrounding seismically qualified components. Although a URM is not allowed by the modern standards for seismic applications, it is found in relatively older NPPs where it has been noted to be a major contributor to the seismic risk (Reed and Kennedy, 1994). The sliding response of objects under seismic excitation has been studied elsewhere (e.g., Konstantinidis and Makris, 2005, 2009, 2010; Konstantinidis and Nikfar 2015; Lin et al. 2015, and references reported therein). The rocking response of a URM frame has been studied by Wesley et al. (1980) where it is considered to be equal to that of a single pier of the frame represented by a Single Degree of Freedom (SDOF) oscillator. ASCE43-05 also provides an approximate method for obtaining the peak rocking response of an unanchored rectangular block by considering it as an equivalent SDOF oscillator. Priestley et al. (1978) proposed a method that leaned on the same asumption, namely that a rocking block can be represented by an equivalent SDOF oscillator. This methodology was evaluated by Makris and Konstantinidis (2003), who reached the conclusion that a rocking block cannot be represented by a SDOF oscillator. The methodology by Westley et al. (1980) was investigated at a preliminary level by Dar et al. (2013) reaching the same conclusion as Makris and Konstantinidis (2003). The ASCE 43-05 approximate methodology was evaluated by Dar et al. (2015b) with the conclusion that this method results in incorrect and in many cases unconservative response of a rocking block. The same conclusion was obtained for this method in the Canadian context with regard to the response spectrum recommended by the standard CSA N289.3 (2010) by Dar et al. (2015d).

All of the above studies aimed at obtaining the pure planar response of a rocking block without sliding. The standard ASCE 43-05 allows independent calculations of pure planar rocking and pure sliding response of an unanchored block. This paper focuses on the pure planar rocking response of frames. Figure 2(a) shows a rocking frame consisting of two rigid unanchored rocking piers with a freely supported rigid beam on top, all components with rectangular shapes having uniform mass distribution. Sufficient friction, and hence no sliding, at contact points (at the top and the bottom of a pier) is assumed. In this type of rocking frame, for positive rotation ($\theta>0$), i.e., rocking motion towards right (shown in Figure 2(a)), the top pivot point, i.e., the contact point of the beam with the pier, is at the pier's top left corner whereas the bottom pivot point is at the bottom right corner of the pier. For negative rotation (motion to the left), the top pivot point switches to the top right corner of the pier and the bottom pivot point switches to the bottom left corner of the pier. The switch takes place instantaneously at the time of impact. Figure 2(b) shows a typical pier just after and just before the impact. Thus the contact point, and hence the lumped mass (mass of the beam divided by the number of piers), always remains at the top end of the diagonal of the pier, i.e., in alignment with the Center of Gravity (CG) of the pier and the bottom pivot point. Thus, the slenderness of the equivalent block, represented by the angle, α, remains the same as that of the solitary pier. This type of rocking frame has been analyzed by Makris and Vassiliou (2013) concluding that the rocking frames can be considered as an equivalent rocking block shown in Figure 2(c), with the same slenderness as that of the rocking pier but of a larger size (because the CG of the pier-beam assembly would be higher than the CG of the individual pier).

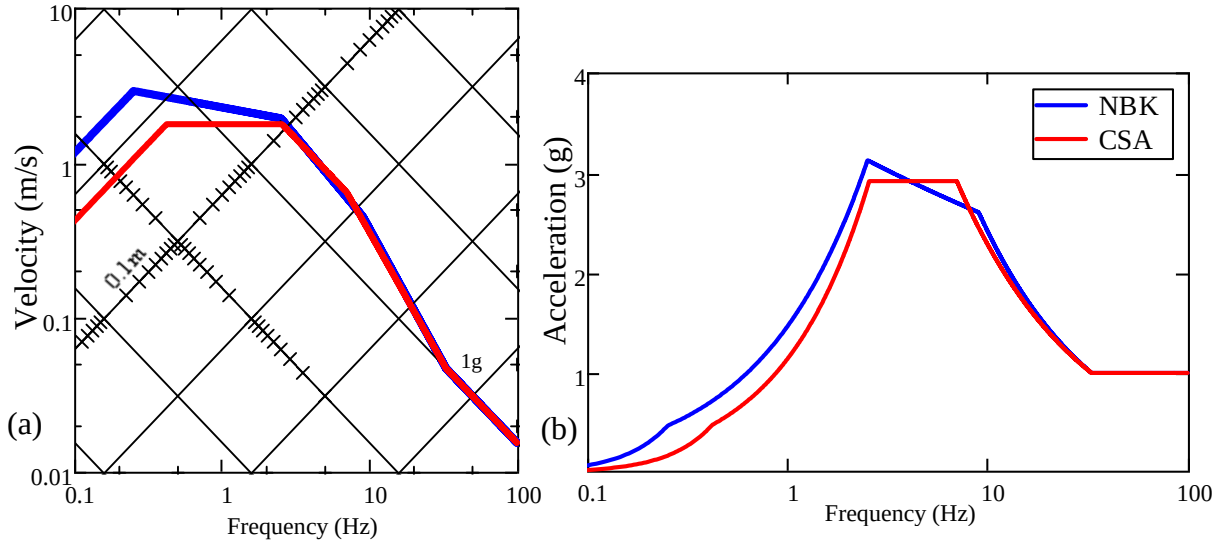

Figure 1: NBK spectrum (USNRC RG 1.60) and CSA spectrum (CSA N289.3) at 5% damping, normalized to 1g PGA with: (a) spectral velocity, displacement and acceleration (b) only spectral acceleration.

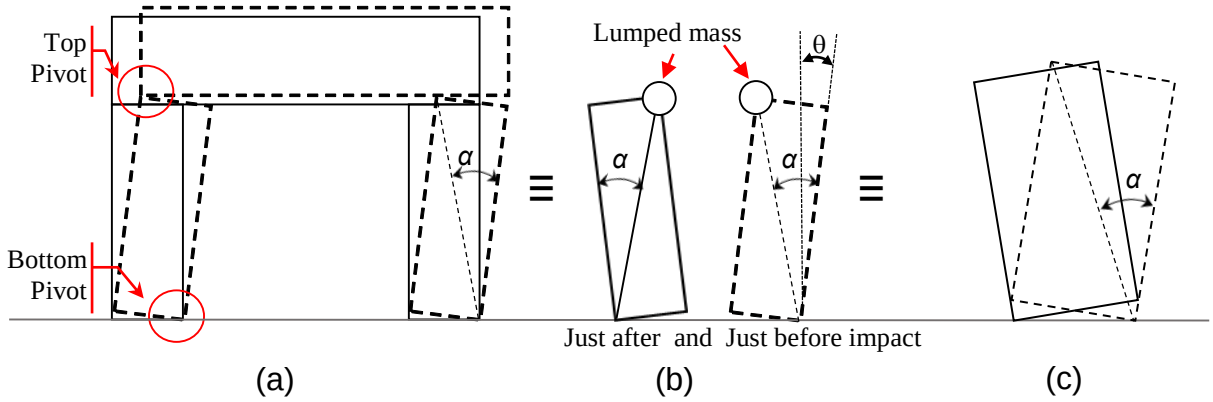

Figure 2: Rocking frame investigated by Makris and Vassiliou (2013): (a) Rocking frame consisting of rigid piers and top beam (b) Rocking pier with lumped mass shifting instantaneously at top pivot point on impact (c) Equivalent rocking block with the same slenderness but larger size.

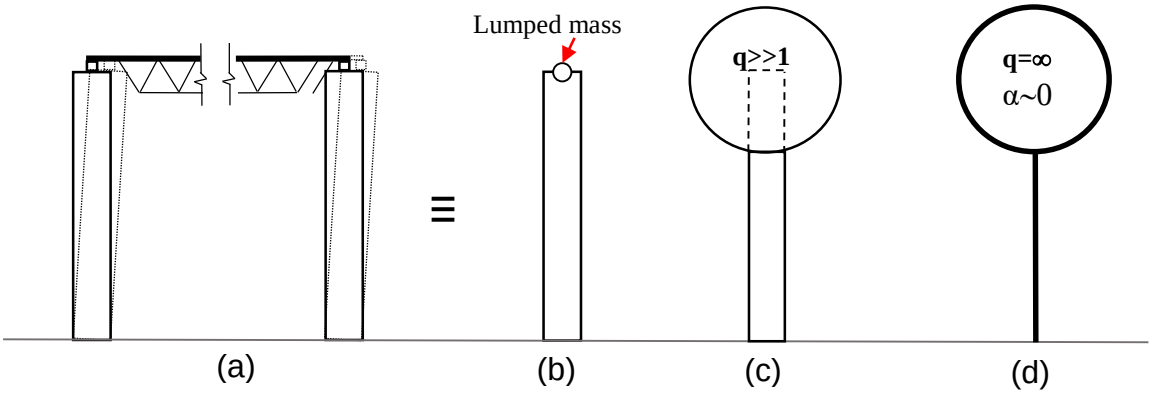

Figure 3: Slender URM rocking frame: (a) Concrete block unreinforced masonry with rigid diaphragm on top connected at the centers of the piers (b) Single pier with lumped mass (c) Pier with very large mass (d) Pier with zero slenderness and infinite top mass

Figure 3(a) shows a slender frame made of URM piers with a rigid diaphragm, made of steel deck and open web steel joists (or steel beams) connected at the piers' top center points. Preliminary investigation of this type of frame was carried out by Dar et al. (2015c). It was concluded that the response of a rocking frame is equal to that of a single pier with a lumped mass, i.e., the mass of the top rigid diaphragm equally divided among piers, as shown in Figure 3(b). As the ratio of the top mass with the pier mass, represented by the letter 'q', increases, the CG moves upwards as shown in Figure 3(c). As α approaches zero and q approaches infinity, the entire arrangement turns into an unstable stick-mass model as shown in Figure 3(d). Parameters of an equivalent rectangular block, representing the assembly in Figure 3(b) were established by Dar et al. (2015c) which are revisited in this paper. It is assumed that sufficient friction exists at all contact points at the top and bottom of the URM. Hence there is no sliding. The support offered by the URM is considered as a line support, referred as "point of contact". The URM piers are considered as rigid rocking blocks, henceforth referred to as solitary blocks. The effects of the joist shoe and bearing plate (about 100 mm x 100 mm in plan) and its anchor are ignored.

2. REVIEW OF THE ROCKING BLOCK

Figure 4(a) shows the schematics of a rocking block subject to ground excitation $\ddot{x}_g$. Yim et al. (1980) presented the equations of motion of the rocking block,

$$[1]\quad I\ddot{\theta} + mgR\sin(-\alpha - \theta) = -m\ddot{x}_g R\cos(-\alpha - \theta), \quad \theta < 0$$

$$[2]\quad I\ddot{\theta} + mgR\sin(\alpha - \theta) = -m\ddot{x}_g R\cos(\alpha - \theta), \quad \theta > 0$$

Where, I is the moment of inertia of the rocking block about the pivot point O, m is its mass, R is its radius, θ is the rotation, angle α is the measure of its slenderness. Other parameters are as defined in Figure 4.

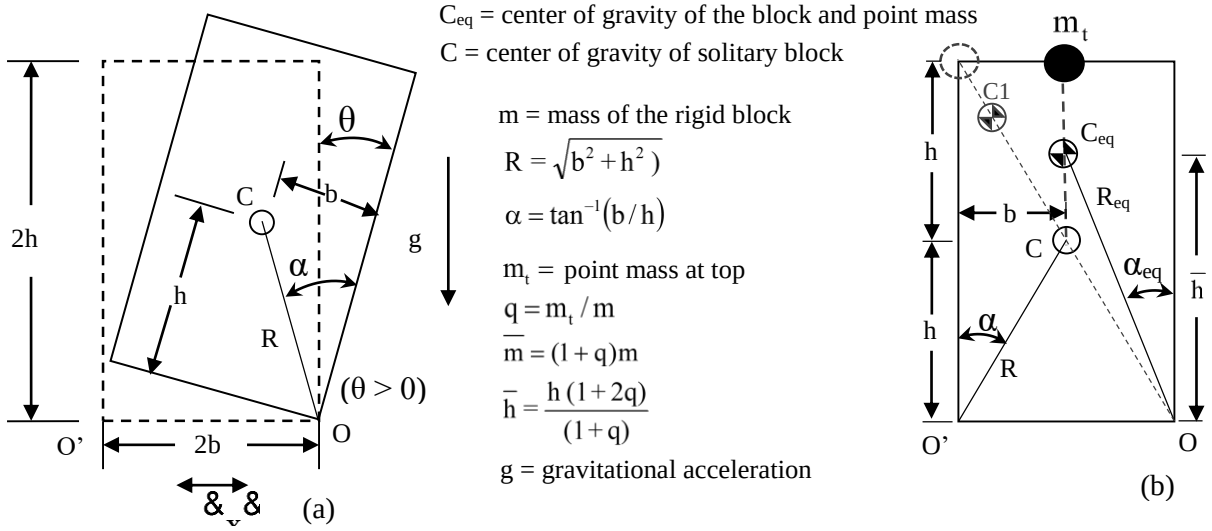

Figure 4: (a) Schematics of a rocking block (b) Equivalent block

Substituting I= (4/3) mR^2 in the above equations and rearranging the terms leads to

$$[3]\quad \ddot{\theta} = -p^2\left[\sin\{\alpha\,\mathrm{sgn}(\theta) - \theta\} + \frac{\ddot{x}_g}{g}\cos\{\alpha\,\mathrm{sgn}(\theta) - \theta\}\right]$$

where, $p = \sqrt{3g/4R}$ is the so called frequency parameter. sgn(θ) denotes the signum function. Employing the space state formulation (Makris and Konstantinidis, 2003), the above equation can be solved numerically by modifying the initial velocity $\dot{\theta}_2$ after each impact by multiplying the pre-impact velocity $\dot{\theta}_1$ by the coefficient of restitution given by Housner (1963) as

[4] $$e = 1 - \frac{3}{2}\sin^2\alpha$$

3. EQUIVALENT ROCKING BLOCK PARAMETERS

There are two extremes for the location of the top lumped mass on a pier, depending on the way the beam is supported on the piers: (1) at the top centers of the piers (Figure 3), and (2) at the corners of the piers (Figure 2). Parameters of the equivalent block, α_{eq} and p_{eq}, are derived below for the two extreme cases. Equivalent parameters for the top mass located between the two extremes are under investigation by the authors. Figure 4(b) shows the rocking block geometry with the top mass (shown as a solid circle) in the center and also at the top left corner as a dotted circle.

4. TOP MASS AT THE CENTER

Regardless of the position of the top mass, the CG of the block (solitary pier) and top mass assembly would be located on the line joining the top mass and the CG of the solitary block, which is denoted as point C and highlighted by a small circle in Figure 4(b). For the centrally located top mass (solid circle), m_t, and block mass m, the height of the point C_{eq} is

[5] $$\bar{h} = h + \frac{hq}{1+q} = \frac{h(1+2q)}{(1+q)}$$

The distance of point C_{eq} from the point O and the angle α_{eq} come out to be

[6] $$R_{eq} = R\left(\sin^2\alpha + \cos^2\alpha\left(\frac{1+2q}{1+q}\right)^2\right)^{\frac{1}{2}}$$

[7] $$\alpha_{eq} = \tan^{-1}\left(\left(\frac{1+q}{1+2q}\right)\tan\alpha\right)$$

The properties of the equivalent rocking block (i.e., the point mass and solitary block assembly), the mass moment of inertia about pivot point O and the frequency parameter, are obtained as

[8] $$I_{eq} = I\left(1 + \frac{3}{4}q\left(1 + 3\cos^2\alpha\right)\right)$$

[9] $$p_{eq}^{\ 2} = \frac{\bar{m}gR_{eq}}{I_{eq}} = p^2(1+q)\frac{\left(\sin^2\alpha + \cos^2\alpha\left(\frac{1+2q}{1+q}\right)^2\right)^{\frac{1}{2}}}{\left(1 + \frac{3}{4}q\left(1 + 3\cos^2\alpha\right)\right)}$$

5. TOP MASS AT THE CORNER

For the mass at the corner (dotted circle in Figure 4(b)), the CG of the equivalent block (solitary block and top mass assembly) would be at the diagonal (at point C1) and hence the angle α_{eq} would be equal to α. By proportioning the distance from the point C of the top corner mass in accordance with the mass ratio (as in Eq. 5), the following relationships emerge

[10] $R1_{eq} = R + \frac{Rq}{1+q} = \frac{R(1+2q)}{(1+q)}$ is the distance between the points C1 and O.

[11] $I1_{eq} = \frac{4}{3}mR^2 + 4m_t R^2 = I(1+3q)$

[12] $p1_{eq}^{\ 2} = \frac{\overline{mg}R1_{eq}}{I1_{eq}} = p^2\left(\frac{1+2q}{1+3q}\right)$

Out of the above parameters, α_{eq} (= α) and $p1_{eq}$ are the same as those derived by Makris and Vassiliou (2013); however the expression for $R1_{eq}$ derived by Makris and Vassiliou (2013), and denoted by $\hat{R}$, is:

[13] $\hat{R} = R\left(\frac{1+3q}{1+2q}\right)$

As q approaches infinity, the equivalent radius given by Eq. 10 approches 2R, which is also obvious geometrically (Figure 4(b)). $\hat{R}$ in Eq. 13, however, approaches 3/2. This is because the equation for the equivalent radius $\hat{R}$ in Makris and Vassiliou (2013) was derived from the parameter $p1_{eq}$ by equating it to $\sqrt{3g/4R1_{eq}}$. It should be noted that the coefficient ¾ is for a rectangular block with uniformly distributed mass rather than the assembly of a solitary block and the top point mass. Figure 5(a) shows the difference between the equivalent radii, $R1_{eq}$ and $\hat{R}$, from this study and Makris and Vassiliou (2013), denoted as M&V (2013). Figure 5 (a) shows that the size of the equivalent block is more than the size of the solitary block for both. Since response of larger blocks is less than the response of smaller blocks, it appears that the top heavy frames are more stable than a solitary block. However, it is not necessarily true in all cases, as seen later.

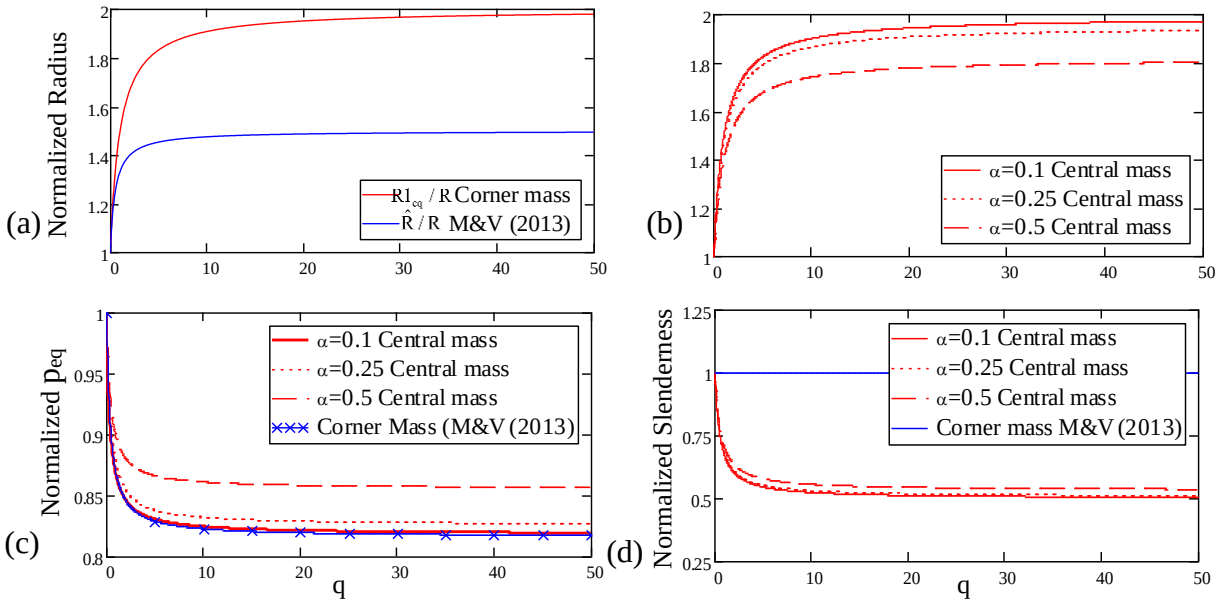

Figure 5: Parameters of an equivalent block: (a) Normalized radius $R1_{eq}/R$ for the top mass at corner (b) Normalized radius R_{eq}/R for the centrally located top mass (c) Normalized $p_{eq}=p_{eq}/p$, and, (d) Normalized slenderness α_{eq}/α.

6. PARAMETRIC STUDY OF THE TWO EXTREME CASES

Figure 5 (b) shows that the variation in the normalized radius against variation in q of a block with centrally located top mass. As slenderness decreases, the shape of the curve (e.g., the top curve with α=0.1), asymptotes to 2, similar to that in Figure 5 (a) for the corner top mass. This means that for slender rocking frames the equivalent radius for both cases is almost the same. This is true for all parameters shown in Figure 5 except for the normalized slenderness in Figure 5(d) where, for small α, for the central mass case, it asymptotes to 0.5 but for the corner mass it stays constant at 1. This can be realized geometrically from Figure 4(b) that for the centrally located mass for slender frames with $q=\infty$, $\alpha_{eq}=b/2h$ whereas $\alpha=b/h$.

7. MAXIMUM COEFFICIENT OF RESTITUTION

Figure 6 (a) and (b) show the rocking block just after and just before the impact at point O'. For a rectangular block with uniformly distributed mass, Housner (1963) considered the following relationship, derived by equating angular momentum about point O' immediately before and after the impact, in order to arrive at the coefficient of restitution given in Eq. 4:

$$[14] \quad (I - 2mbR\sin\alpha)\dot{\theta}_1 = I\dot{\theta}_2$$

Adding the effect of the top mass on both sides of the equation (with the velocities v_v and v_h from Figure 6), just before and after the impact,

$$[15] \quad \left[(I - 2mbR\sin\alpha)\dot{\theta}_1 + m_t v_h(2h) - m_t v_v(b)\right]_{before} = \left[I\dot{\theta}_2 + m_t v_h(2h) + m_t v_v(b)\right]_{after}$$

The above leads to the coefficient of restitution

$$[16] \quad e_{eq} = \frac{\dot{\theta}_2}{\dot{\theta}_1} = \frac{e + \frac{3}{4}q\left(5\cos^2\alpha - 1\right)}{1 + \frac{3}{4}q\left(3\cos^2\alpha + 1\right)}$$

Where e is given in Eq. 4.

Similarly, the coefficient of restitution can be found for the point mass at the top corner by replacing R_1 by 2R in Figure 6 . This comes out to be the following:

$$[17] \quad e1_{eq} = \frac{e + 3q\cos(2\alpha)}{1 + 3q}$$

The above is the same as given by Makris and Vassiliou (2013).

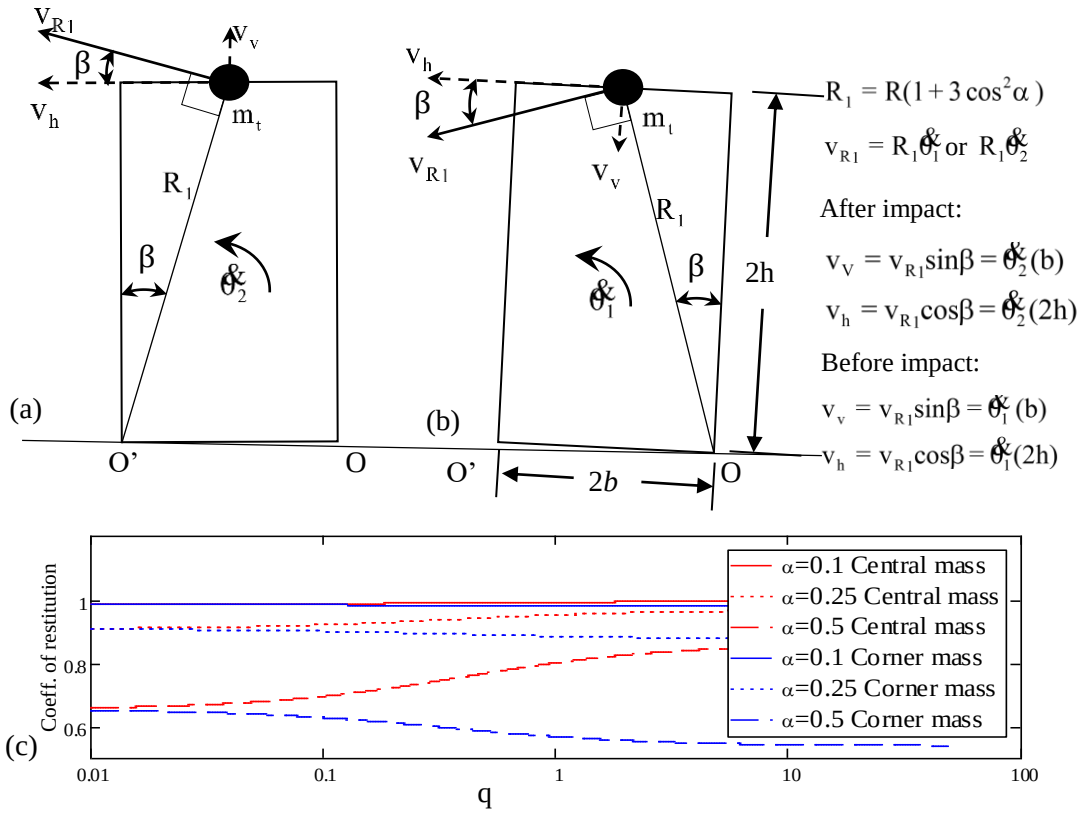

Figure 6: Rocking block with top central mass: (a) just after, and, (b) just before, impact. (c) variation in coefficient of restitution with q

Figure 6 (c) shows the variation in coefficient of restitution with increasing q on log-linear scale. All red lines correspond to the block with top central mass, and all blue lines correspond to the block with the top corner mass. The coefficient of restitution increases with the increase in q for the top central case whereas it decreases for the top corner case for all three values of α. For α=0.1, the coefficient of restitution for both cases is almost the same as of the solitary block.

8. RESPONSE OF A SLENDER ROCKING FRAME TO EARTHQUAKE RECORDS

A 3m high and 290mm thick concrete URM supporting a roof diaphragm spanning 6 m, similar to what is shown in Figure 3 is considered. Unit area roof diaphragm weight is considered as 75% of the masonry self-weight leading to q=0.75, which is not uncommon to such enclosures. Table 1 gives details of this rocking frame along with the equivalent block parameters in the last three columns. Four earthquake records are chosen, as shown in Table 2. Overturning is assumed to occur when the normalized rotation (θ/α or θ/α_{eq}) is equal to 1, although it is known that a rocking block may survive rotations that exceed this limit (Zhang and Makris, 2001).

Table 1: Details of block wall and diaphragm system for centrally loaded frames

h (mm)	b (mm)	R (mm)	q	α (Radian)	p (Radian/s)	e	α_{eq} (Radian)	p_{eq} (Radian/s)	e_{eq}
1500	145	1507	0.75	0.096	2.209	0.986	0.068	1.94	0.992

Table 2: Details of Earthquake Records

Earthquake	Year	Station	PGA (g)	Record
Saguenay, Quebec	1988	Site 16	0.13	*S16_EN2
Helena	1935	Carroll College	0.173	A-HMC-270
Imperial Valley, Calif.	1940	El Centro	0.215	I-ELC270
San Fernando, Calif.	1971	Pacoima Dam	1.16	PCD 254

http://peer.berkeley.edu/smcat/ and *http://www.earthquakescanada.nrcan.gc.ca

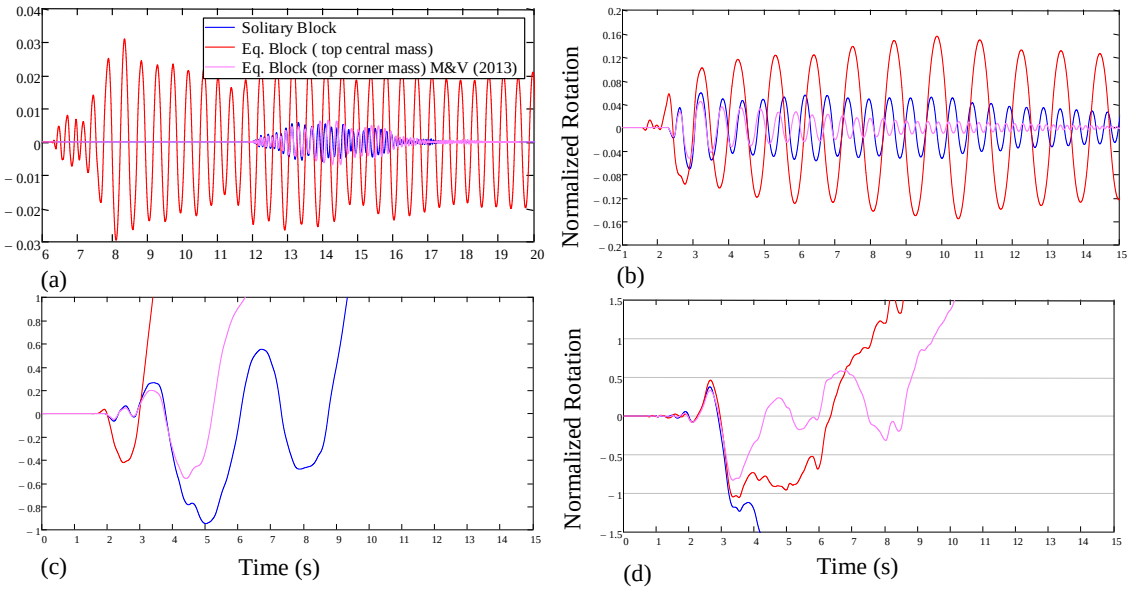

Figure 7: Response of solitary and equivalent rocking blocks to earthquake records in Table 2: (a) Saguenay (b) Helena (c) El Centro (d) San Fernando

Response of a rectangular block to seismic excitation is obtained by numerically solving Eq. 3 utilizing the space state formulation (Makris and Konstantinidis, 2003) and employing AdmsBDF hybrid solver (PTC, 2012). Figure 7 shows the response of solitary block in comparison with that of the corresponding equivalent rocking block to the earthquake records detailed in Table 2. Three cases are considered: solitary block, equivalent block with top central mass, and equivalent block with top corner mass. As shown in Figure 7(a) and (b) there is no overturning, and the response of the equivalent block with the centrally located top mass is much more than the other two cases. The response of equivalent block with the corner top mass is the least of all. This means that the equivalent block with the top corner mass is the most stable. However, in Figure 7(c), where there is overturning, the response of solitary block is more stable than the other two cases. In Figure 7(d), the solitary block is the least stable and the equivalent block with top corner mass is the most stable of all. From this observation it can be concluded that for rotations closed to overturning, the top heavy frame may not be more stable than a solitary block, although the size of an equivalent block is larger than the corresponding solitary block. This is also visible in various rocking spectra generated by Makris and Konstantinidis (2003) where, when close to overturning, for two values of p close to each other, the response of a smaller block in many cases is found to be less than that of a larger block. As given in Table 1, parameters p_{eq} and p are close to each other and hence the rocking response, corresponding to these parameters, appear to follow the observations made in the literature.

9. CONCLUSIONS

It is concluded that the parameters of an equivalent rocking block depend on the boundary conditions at the contact points of piers and the top rigid beam (or a diaphragm) in a rocking frame. For both cases, with the top mass located at the center and corner of a pier, the size of an equivalent block is larger than that of the solitary block. However, the slenderness parameter, α, for the centrally loaded pier is less than that of the solitary block whereas for the top mass at the corner of a rocking pier, the slenderness parameter is equal to that of a solitary block. A preliminary investigation with seismic input from a limited number of earthquake records concludes that, when close to overturning condition, the top heavy slender frames are not necessarily more stable than the corresponding solitary blocks.

REFERENCES

Alexander, C. M., Baughman, P. M., and Brown, G. N. 2007. Seismic Margin Assessment in Ontario Nuclear Power Plants. *Transactions of the 19th International Conference on Structural Mechanics in Reactor Technology (SMiRT 19).* Toronto, Canada.

American Society of Civil Engineers. 2005. *ASCE 43-05 – Seismic Design Criteria for Structures, Systems and Components in Nuclear Facilities.* Reston, Virginia, USA.

Atkinson, G. M., and Elgohary, M. 2007. Typical Uniform Hazard Spectra for Eastern North American Sites at Low Probability Levels. *Canadian Journal of Civil Engineering*, 34, 12-18.

Boore, D. M., and Atkinson, G. M. 1992. Source Spectra for the 1988 Saguenay, Quebec Earthquakes. *Bulletin of the Seismological Society of America*, 82(2), 683-719.

CSA. 1981, 2010. CSA N289.3. *Design Procedures for Seismic Qualification of CANDU Nuclear Power Plants*. Rexdale, Ontario, Canada: Canadian Standards Association.

Dar, A., Iyengar, R. N., and Chhatre, A. 2015a. Comparison of Seismic Qualification Challenges for Nuclear Power Plants in North America and Peninsular India. *Transactions, 23rd International Structural Mechanics in Reactor Technology Conference (SMiRT23).* Manchester, UK.

Dar, A., Konstantinidis, D., and El-Dakhakhni, W. 2013. Requirement of Rocking Spectrum in Canadian Nuclear Standards. *Transactions, 22nd International Structural Mechanics in Reactor Technology Conference (SMiRT22).* San Francisco, CA.

Dar, A., Konstantinidis, D., and El-Dakhakhni, W. W. 2015b. Evaluation of ASCE 43-05 Seismic Design Criteria for Rocking Objects in Nuclear Facilities. *Journal of Structural Engineering* (In Press).

Dar, A., Konstantinidis, D., and El-Dakhakhni, W. W. 2015c. Seismic Response of Masonry Rocking Frames in Nuclear Power Plants. *Transactions, 23rd International Structural Mechanics in Reactor Technology Conference (SMiRT23).* Manchester, UK.

Dar, A., Konstantinidis, D., and El-Dakhakhni, W. W. 2015d. Shortcomings of the ASCE 43-05 Approximate Method for Estimating the Seismic Demands on Rocking Objects in Canadian Nuclear Power Plants. Proceedings, *The 11th Canadian Conference on Earthquake Engineering.* Victoria, BC, Canada.

EPRI. 1991. NP-6041-SL- Revision 1, *A Methodology for Assessment of Nuclear Power Plant Seismic Margin*, Electric Power Research Institute, USA.

Housner, G. W. (1963). The Behavior of Inverted Pendulum Structures During Earthquakes. *Bulletin of the Seismological Society of America*, 53 (2), 403–417.

Konstantinidis, D., and Makris, N. 2005. *Experimental and Analytical Studies on The Seismic Response of Freestanding and Anchored Laboratory Equipment*. Report No. 2005/07. Berkeley: Pacific Earthquake Engineering Research Center (PEER), University of California.

Konstantinidis, D., and Makris, N. 2009. Experimental and Analytical Studies on the Response of Freestanding Laboratory Equipment to Earthquake Shaking. *Earthquake Engineering and Structural Dynamics*, 38 (6), 827–848.

Konstantinidis, D., and Makris, N. 2010. Experimental and Analytical Studies on the Response of 1/4-Scale Models of Freestanding Laboratory Equipment subjected to Strong Earthquake Shaking. *Bulletin of Earthquake Engineering*, 8 (6), 1457–1477.

Konstantinidis, D., and Nikfar, F. 2015. Seismic Response of Sliding Equipment and Contents in Base-Isolated Buildings Subjected to Broad-Band Ground Motions. *Earthquake Engineering and Structural Dynamics*, 44(6), 865-887.

Lin, S. L., MacRae, G. A., Dhakal, R. P., and Yeow, T. Z. (2015). Building Contents Sliding Demands in Elastically Responding Structures. *Engineering Structures*, 86.

Makris, N., and Konstantinidis, D. 2003. The Rocking Spectrum and the Limitations of Practical Design Methodologies. *Earthquake Engineering and Structural Dynamics*, 32 (2), 265–289.

Makris, N., and Vassiliou, M. F. 2013. Planar Rocking Response and Stability Analysis of an Array of Free-Standing Columns Capped with a Freely Supported Rigid Beam. *Earthquake Engineering and Structural Dynamics*, 42(3), 431-449.

Newmark, N. M., and Hall, W. J. 1978. *Development of criteria for seismic review of selected nuclear power plant NUREG/CR-0098*. United States Nuclear Regulatory Commission.

Newmark, N. M., Blume, J. H., and Kapur, K. K. 1973, November. Seismic Design Spectra for Nuclear Power Plants. *Journal of the Power Division*, ASCE, 99(PO2), 287-303.

Priestley, M., Evison, R., and Carr, A. J. 1978. Seismic Response of Structures Free to Rock on Their Foundations. *Bulletin of the New Zealand National Society for Earthquake Engineering*, 11(3), 141–150.

PTC. (2012). Mathcad 15.0. Parametric Technology Corporation, 140 Kendrick Street, Needham, MA 02494, USA.

Reed, J. W., and Kennedy, R. P. 1994. *Methodology for Developing Seismic Fragilities EPRI TR-103959*. Palo Alto, California: Electric Power Research Institute.

USNRC. 1973. *Design Response Spectra for Seismic Design of Nuclear Power Plants, Regulatory Guide 1.60, Revision 1*. Washington, D.C.: United States Nuclear Regulatory Commission.

USNRC. 2014. *Design Response Spectra for Seismic Design of Nuclear Power Plants, Regulatory Guide 1.60, Revision 2*. Washington DC: United States Regulatory Commission.

Wesley, D. A., Kennedy, R. P., and Richter, P. J. 1980. Analysis of the Seismic Collapse Capacity of Unreinforced Masonry Wall Structures. Proc. *7th World Conference on Earthquake Engineering*. Istanbul, Turkey.

Yim, C. K., Chopra, A., and Penzien, J. 1980. Rocking Response of Rigid Blocks to Earthquakes. *Earthquake Engineering and Structural Dynamics*, 8 (6), 565–587.

Zhang, J., and Makris, N. 2001. Rocking Response of Free-Standing Blocks Under Cycloidal Pulses. *Journal of Engineering Mechanics* (ASCE), 127(5), 473-483.